ASIAN JOURNAL OF CIVIL ENGINEERING (BHRC) VOL. 14, NO. 1 (2013)
PAGES 47-70

FABRICATION AND EXPERIMENT OF A HYDRO-PNEUMATIC SEMI-ACTIVE RESETTABLE DEVICE

A. Keyhani[a], S. M. Sajjadi Alehashem[*,a,b] and Y. Q. Ni[b]
[a]Shahrood University of Technology, Shahrood, Iran
[b]The Hong Kong Polytechnic University, Hong Kong, China

Received: 2 February 2012; **Accepted**: 10 May 2012

ABSTRACT

A new innovative Hydro-pneumatic Semi-active Resettable Device by using MR-Fluid (MR-HSRD) is introduced for vibration suppression of structures. The novel device consists of a cylinder-piston system with control valve and magneto-rheological valve (MR-valve) mounted on a bypass pipe connecting two sides of the cylinder. The MR-HSRD is set by changing the stiffness and the damping of the device independently. Moreover, the hysteresis behavior can be adjusted by using different control logics for control valve. A mathematical model is presented for behavior of the device. The experimental results of MR-HSRD under cyclic and static loadings are presented and are compared with the mathematical models.

Keywords: semi-active control; resettable device; variable stiffness; MR-fluid; MR-valve; hydro-pneumatic actuator

1. INTRODUCTION

Semi-active control of structures offers two main benefits over active and passive control. First, a large power/energy supply is not required. Second, semi-active systems provide the broad range of control that a passive system cannot. These two features make them an alternative to both passive and active control. A comprehensive literature about semi-active control systems can be found in reference [1].

The heart of a semi-active control system is the semi-active control device. Resettable devices are among semi-active devices. A resettable device usually consists of a hydraulic cylinder-piston system with a bypass valve connecting two sides of the cylinder [2]. Resettable devices act as hydraulic or pneumatic springs, resisting displacement in both direction and their un-stretched spring length can be reset to extract maximum energy

* E-mail address of the corresponding author: m_sajjadi_a@yahoo.com (S. M. Sajjadi Alehashem)

dissipation from the excited structure [3]. However, they possess the ability to store the vibration energy and dissipate/release the stored energy at appropriate time. The control logic of a resettable device is often aimed at finding suitable time for reducing the stiffness (resetting the device by opening the control valve) and then increasing it back to the high value (by closing the control valve). Up to now, different types of resettable devices have been proposed and studied for possible application to the vibration control of structures. Bobrow *et al.* [3] proposed and studied a hydraulic resettable actuator. Kurino *et al.* [4] developed a switching semi-active oil damper that is able to dissipate energy twice an ordinary passive damper. They also developed a passive device with semi-active characteristics [5]. Chase *et al.* [6] proposed a two-chambered resettable device that utilizes each chamber independently. In this device air is used as the working fluid and the surrounding atmosphere have been used as the fluid reservoir. A new adaptive passive fluid spring and damper (ASD) is proposed and tested by Nagarajaiah *et al.* [7]. The ASD is capable of varying the stiffness and damping independently. Many researchers have studied the resettable actuators similar to the one studied by Bobrow with pressured gas as working fluid [2, 8-11]. The effect of hydraulic resettable actuator in seismic response control of structures is also investigated [3, 12-15]. In the literature, the effects of two-chambered resettable device in response to seismic loads have evaluated [16-21]. Moreover, a nonlinear model for this kind of resettable devices is proposed by Mulligan *et al.* [22,23] and validated by experiments. The control approaches for structures equipped with semi-active variable stiffness devices are also studied [10, 16, 24-27].

It has been demonstrated, through extensive simulations and experimental studies that the resettable devices possess promising performance in suppression vibration response of structures [2, 8, 10, 12-14, 17, 28-30]. However, the studied resettable devices have some limitations and shortcomings. A resettable device with small capacity (approximately about 100N) was tested by Jabbari and Bobrow [2]. It offers the capability of releasing all the stored energy effectively in a short time. Generally, for devices with larger capacity the rate of energy dissipation may be more critical as the required flow rates to release large amounts of stored energy will potentially be very high. Hence, the energy dissipating time maybe significant in comparison with the structural response. Previous results of experiments carried out on two-chambered resettable devices with air as working fluid showed some limitations in their energy dissipation capacity for high frequency excitation [23, 31, 32]. Moreover, for higher resistance force, discharging the air through the valves to dissipate the stored energy requires a significant times for some test cases [6, 23, 31, 32]. Unsymmetrical behavior of device is observed due to decentralizing the piston [6, 32, 33] that is probable to be happened during installation of device in the structure. In addition, because the pressure of gas in two-chambered semi-active resettable device is equal to the pressure of atmosphere, so the resistance force and stiffness of the device are limited and cannot be changed [32]. However, the idea of connecting high-pressure tank to the active chamber of device to increase the resistance force and overcome this limitation is proposed by [31, 32] but it cause other difficulties and complexities in device [32]. This paper presents an innovative hydro-pneumatic resettable device by using MR-fluid to overcome the prescribed shortcomings of the current resettable devices.

In the resettable devices, dissipation of stored energy usually occurs by flow of the

working fluid (gas or oil) through a control valve due to pressure difference between the chambers of device. The controllable valve can alter the amount of dissipation of the stored energy. The main goal in the resettable device is to dissipate the stored energy as soon as possible preventing release of the stored energy to the structure. Therefore, the mechanism of energy dissipation is very important. If the device cannot dissipate the energy rapidly, then the efficiency of resettable device decreases.

In the proposed novel device as shown in Figure 1, a different mechanism is utilized for dissipating the stored energy. The proposed device is a hydro-pneumatic actuator that utilizes two working fluids (i.e. pressurized gas and MR-fluid). The pressurized gas works as a spring and when the control valve is closed, the device serves as a stiffness element in which the stiffness is provide by the bulk modulus of the pressurized gas. Energy dissipation occurs by flowing MR-fluid through the external bypass MR-valve. In this paper, experimental tests on the MR-HSRD have been reported and the relation between the device stiffness and the gas pressure and the length of the gas reservoir is established. The correlation between the experimental results and that of the theoretical ones has been assessed. Experimental results are also used to obtain the relation between the stiffness of MR-HSRD and the gas pressure and the initial length of the gas reservoir.

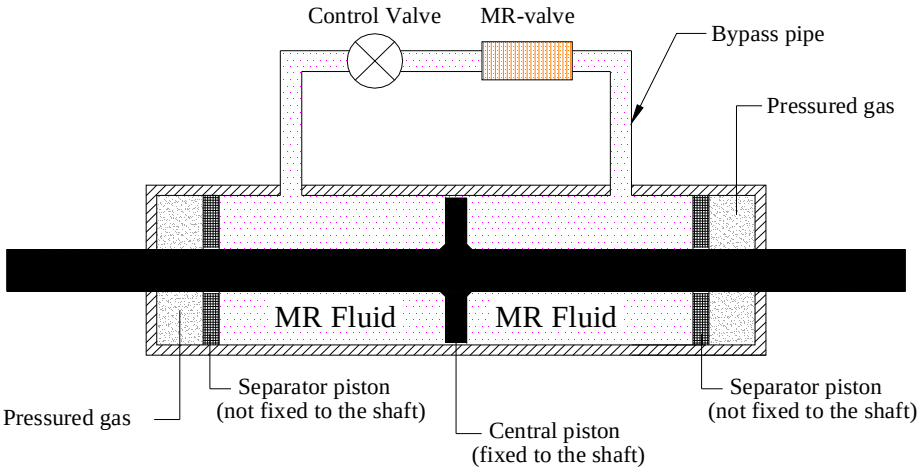

Figure 1. Schematic of the proposed device

2. HYDRO-PNEUMATIC SEMI-ACTIVE RESETTABLE DEVICE BY USING MR-FLUID

The novel resettable device consists of a cylinder-piston system with a control valve as well as a MR-valve mounted on a bypass pipe that connected two sides of the cylinder. The schematic of the proposed device is shown in Figure 1. The cylinder is filled with MR-fluid and pressured gas separated by a movable piston. The pressured gas performs as a spring and by changing either the gas pressure or the initial length of the gas reservoir, the stiffness of the device is adjusted. The MR-fluid and MR-valve perform as energy dissipater.

MR-fluid is a controllable fluid that responds to an applied magnetic field with a

dramatic change in its rheological behavior. The essential characteristic of MR-fluid is the ability to reversibly change from a free flowing, linear viscous liquid to a semi-solid having a controllable yield strength in milliseconds when exposed to a magnetic field. Normally, this change is appeared as a large change in the resistive force of devices in which MR-fluid is used. The MR-fluid is utilized in proposed device to achieve the maximum energy dissipation during device resetting. When the device is excited, the input energy is stored in the pressured gas. Resetting the device by opening the control valve at the due time releases the stored potential energy in the pressured gas and pushes the MR-fluid to flow across the MR-valve to other side of the cylinder. At this time, by changing the shear yield stress of MR-fluid in few milliseconds (by changing the electrical current/voltage in MR-valve) most part of the stored energy dissipates as heat transfer.

The special configuration of the proposed resettable device can produce a large control action by changing its dynamic characteristics. Air is used as working gas in this device and the pressure of gas could be adjusted easily. Stiffness of the device is adjusted by changing the gas pressure or the length of gas reservoir. Also, the damping of the device is adjustable by changing the electrical current/voltage in MR-valve. Moreover, setting the control valve could change the hysteresis behavior. Therefore, stiffness, damping and the hysteresis behavior of the novel device all are controllable.

In developing the force-displacement relationship for the device, when the control valve is closed, the volume of the gas reservoir in each chamber can be related to the piston displacement which in turn leads to a change in the pressure and resistive force. In the novel device, both gas and MR-fluid resist against piston movement and so are important in the resistant force of the device. First, the effect of gas is considered. In the case of an ideal gas (i.e. air) as the working gas, the following equation can be written:

$$p_G V_G^{\gamma} = c \tag{1}$$

Where γ is the ratio of specific heats (γ=1.4 for air), c is a constant, and p_G and V_G are the pressure and volume of the gas in chambers of the device, respectively. Assuming that the initial pressure of gas p_{0G}, and the initial volume V_{0G}, are equal in both chambers, the resistive force of the pressured gas is a function of piston displacement (x) and could be written as:

$$F_G(x) = (p_{2G} - p_{1G})A = [(V_{0G} - Ax)^{-\gamma} - (V_{0G} + Ax)^{-\gamma}]Ac \tag{2}$$

Where, A is the piston area, p_{1G} and p_{2G} are the pressure of chamber1 and chamber2 after displacement, respectively. Expanding the right hand side of Eq. (2) and keeping the linear part, the approximate force is:

$$F_G(x) = -\frac{2A^2 \gamma p_{0G}}{V_{0G}} x \tag{3}$$

Indeed the Eq. (3) shows a linear force-displacement relationship. The effective stiffness of the pressured gas, K_G, is readily defined as:

$$K_G = \frac{2A^2 \gamma p_{0G}}{V_{0G}} \tag{4}$$

If MR-fluid is a compressible liquid (e.g. water, oil, silicon) then the resistance force and the stiffness of the MR-fluid depend on the bulk modulus. For many fluids, the pressure-volume relationship is linear and may be characterized by a proportionality constant called the bulk compressibility modulus, κ. The relationship between a change in pressure (Δp) and the corresponding change in specific volume for MR-fluid, $\Delta V/V_{0MR}$, is written as:

$$\Delta p = -\kappa \frac{\Delta V}{V_{0MR}} \tag{5}$$

Where, V_{0MR} is the initial volume of MR-fluid in the chamber. The minus sign is necessary because a positive change in pressure (a pressure increase) results in a negative change in volume (a volume decrease). Considering the pressure change in MR-fluid on both sides of the piston, the resistive force of MR-fluid is:

$$F_{MR}(x) = 2\Delta pA \tag{6}$$

Where, A is the piston area. By assuming a negative change in the volume of MR-fluid due to compression and by substitution of Eq. (5) in Eq. (6), leads to:

$$F_{MR}(x) = \frac{2\kappa A^2}{V_{0MR}} x \tag{7}$$

And the effective stiffness of the MR-fluid will become:

$$K_{MR} = \frac{2\kappa A^2}{V_{0MR}} \tag{8}$$

The MR-fluid and pressurized gas work as two springs connected in series. Hence, the total stiffness of the device is:

$$K_D = \frac{K_G K_{MR}}{K_G + K_{MR}} \tag{9}$$

As the bulk compressibility modulus (κ) is very large for MR-fluid, so the stiffness of the MR-fluid is much bigger than stiffness of the gas ($K_{MR} >> K_G$) and the stiffness of the device could be written as:

$$K_D \cong K_G \tag{10}$$

Rewriting Eq. (4) in terms of device dimensions lead to a linear stiffness for the device:

$$K_D = K_G = \frac{2(\pi D^2/4)^2 \gamma p_{0G}}{[(\pi D^2/4)L_{0G} + V_{con}]} \tag{11}$$

Where D is the diameter of the piston, L_{0G} is the initial length of the gas reservoir that can be initially set to different values by adjusting the location of the separator pistons to the proper location, and V_{con} is the constant volume in the air reservoir (e. g. volume of air trapped in the connections of the cylinder head and etc.).

To develop a nonlinear mathematical model for the device behavior and to obtain an accurate model, with rewriting Eq. (2) and expanding the right hand side of Eq. (2) and ignoring the parts with order higher than three, the approximate nonlinear force-displacement relation can be written as:

$$F_D(x)_{Nonlin} = F_G(x)_{Nonlin} = \frac{2(\pi D^2/4)^2 \gamma p_{0G}}{[(\pi D^2/4)L_{0G} + V_{con}]} x + \frac{(\pi D^2/4)^4 (\gamma+1)(\gamma+2) p_{0G}}{3[(\pi D^2/4)L_{0G} + V_{con}]^3} x^3 \tag{12}$$

Depend on the ratio of piston displacement to the initial length of the gas reservoir (x/L_{0G}), Eq. (11) and Eq. (12) both can be used to model the pressure-stiffness relation of the device and will be discussed later.

L_{0G} is the initial length of the gas reservoir that can be initially set to different values by adjusting the location of the separator pistons on the shaft. Hence, it can be used to parameterize the design space to determine the appropriate device configuration. This is one of the particular characteristics of the novel device that the previous resettable devices lack. Moreover, the maximum stroke of the piston can be adjusted according to the predicted displacement in the structure just by changing the initial length of the gas reservoir (L_{0G}) and consequently by changing the initial volume of MR-fluid (V_{0MR}), not by changing the whole device necessarily. The relationship between the device dimensions, initial pressure of gas and stiffness of the device according to Eq. (11) is shown in Figure 2 for p_{0G}=500 kN/m^2. As it is shown in Figure 2, with a constant diameter for the piston (D), a wide range of stiffness is available from low stiffness to very high stiffness either by changing the initial length of the gas reservoir (L_{0G}) or initial pressure of gas (p_{0G}). This is an advantage of the proposed device that can be attributed to its special utilization of two gas chambers with separator pistons. Also by using separated gas reservoir in special configuration in the novel device, gas reservoirs can work as accumulator of the common fluid dampers. So, desirable stiffness can be achieved by changing the pressure of gas without needing any accumulator. Furthermore, unlike the previous types of the resettable devices, the proposed device is insensitive to centralizing main piston during the installation of MR-HSRD in the structure and it can behave completely symmetric in both directions. This is a unique feature of the device. It is attributed to the fact that during installation (while the control valve is open); the volume and the pressure of gas are equal in the both chambers irrespective of the position of main piston. Beside the unique benefits of MR-HSRD, it is a fail-safe device and it can serve as an ordinary passive damper when the control valve and/or MR-valve failed.

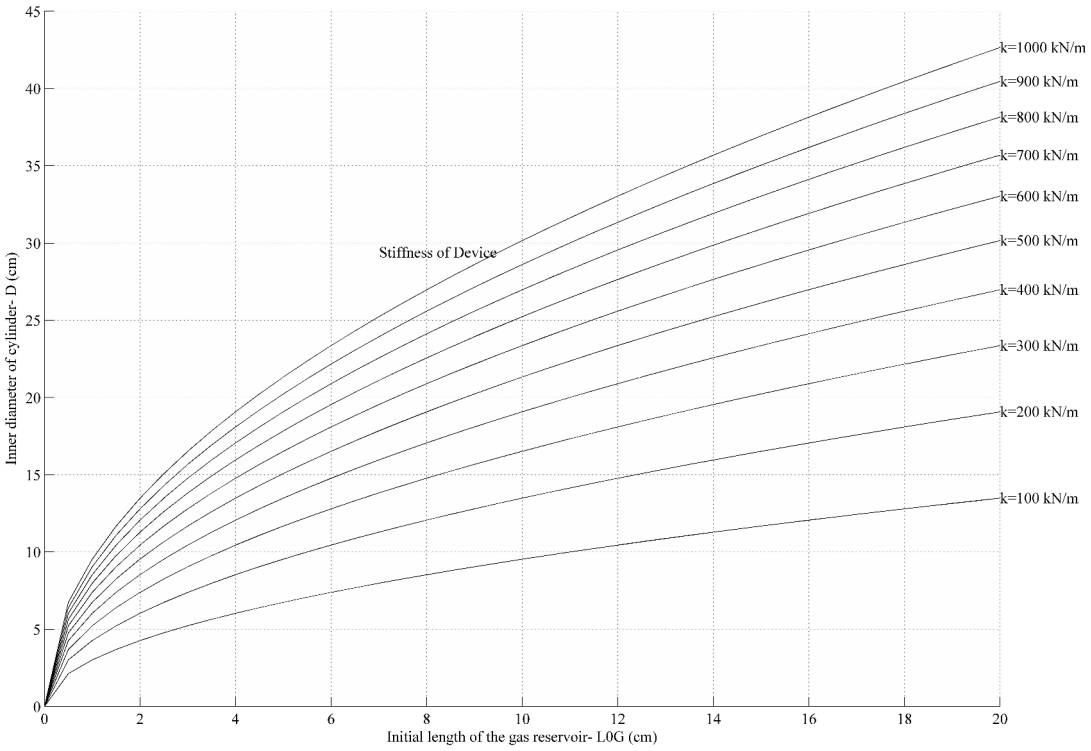

Figure 1. Relationship between the device dimensions and device stiffness for p_{0G} = 500 kN/m^2

3. ENERGY DISSIPATION MECHANISM

Magneto-rheological fluid (MR-fluid) is a type of smart fluid that its rheological properties change when subjected to a magnetic field. Rheological properties are related to the deformation and flow of a material, including elasticity, plasticity, and viscosity. In the case of MR-fluid, the shear yield stress of the fluid (the point after which the fluid flows freely) can alter from zero (a Newtonian fluid) to some finite value (a non-Newtonian fluid). This change in rheological properties is induced by application of a magnetic field to the fluid. The change is completely reversible and occurs within milliseconds. MR-fluid consists of a carrier fluid, which is usually water or some type of oil, with micron-sized magnetic particles suspended in it. The magnetic particles usually compose 20-40% of the volume of the fluid [34]. Commercially available MR-fluid also contains some type of additives to keep the particles suspended in the fluid. In the absence of a magnetic field, MR-fluids exhibit Newtonian behavior and under shear stress MR-fluid flows just as the carrier fluid. The flowing fluid follows the equation:

$$\tau = \eta\dot{\gamma} \tag{13}$$

Where τ is the shear stress, η is the viscosity of the carrier fluid, and $\dot{\gamma}$ is the shear strain rate. This relates to the off-state of the MR-fluid (when there is not any magnetic field).

When a magnetic field is applied, the magnetic particles in the fluid align with the magnetic flux lines and interaction between the resulting induced dipoles causes the particles to form chain-like structures, parallel to the applied field (Figure 3). These chain-like structures restrict the motion of the fluid, thereby increasing the viscous characteristics of the suspension and significantly increasing the fluid's resistance to flow. The fluid does not flow until the shear stress applied reaches a threshold value (the shear yield stress of the fluid), after which the fluid flows. The yield stress increases as the applied magnetic field increases, resulting in a field dependent shear yield stress.

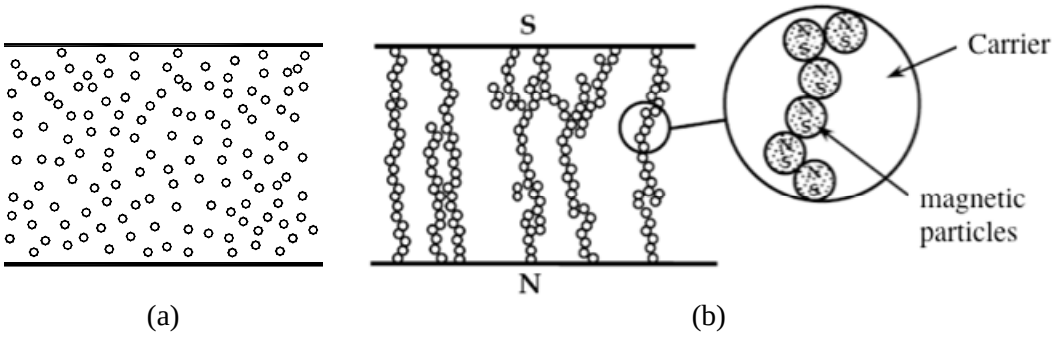

Figure 2. Dipole alignments of magnetic particles in MR-fluid; a) Off-state of fluid (in absence of magnetic field), b) On-state of fluid (with magnetic field) [35]

The nonzero yield stress makes the MR-fluid as a non-Newtonian fluid. The behavior of the fluid is described by the Bingham's equation:

$$\tau = \tau_y(H) + \eta\dot{\gamma} \tag{14}$$

Where $\tau_y(H)$ is the shear yield stress of the fluid. In Eq. (14), when the shear stress surpasses the shear yield stress of the fluid, the fluid flows. This is referred to the on-state of MR-fluid. A simple Bingham plasticity model is shown in Figure 4 that describes the essential field dependent fluid characteristic. Aside from simply being on or off, the MR-fluid can obtain a shear yield stress anywhere in a range by varying the strength of the applied magnetic field. The response time of the fluid to change its properties once a magnetic field is induced is about a few milliseconds.

There are two main modes that MR-fluid can operate in the devices that utilized it [36]. In both modes, the fluid is between two parallel plates that serve as the poles for the magnetic field. The first mode is known as direct shear mode (Figure 5(a)). In this mode, the plates are moving relative to each other. Shear mode dampers are typically used for low-force applications. The second mode is flow mode, also known as valve mode (Figure 5(b)). In this mode, the plates are stationary, and pressure drives the fluid flow. Flow mode devices are capable to produce very high forces, but are more difficult to design.

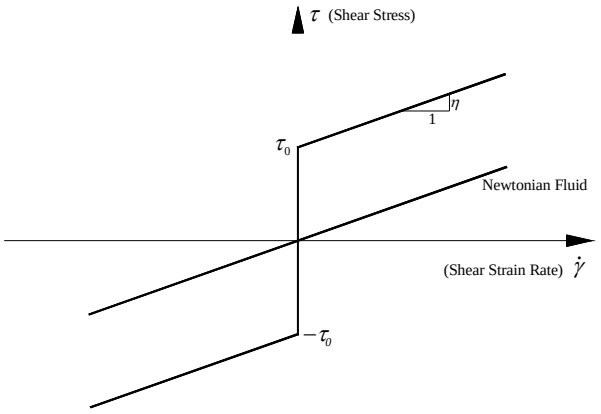

Figure 3. Bingham plasticity model

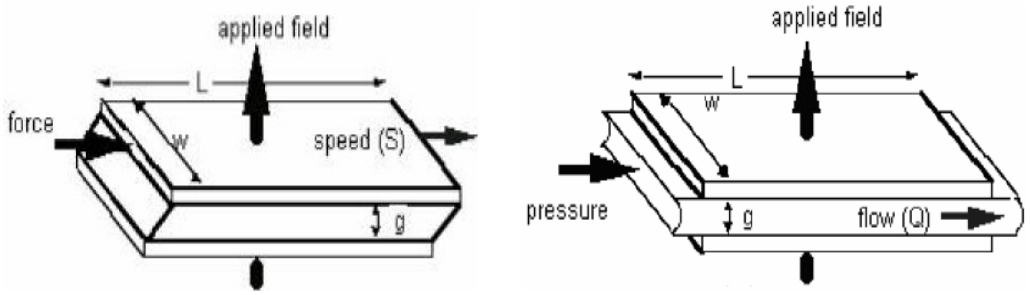

(a) (b)

Figure 4. Shear modes in MR-fluids; (a) Direct shear mode, (b) Pressure driven flow mode [36]

In the proposed MR-HSRD (Figure 1), the MR-valve performs as an energy dissipater. In fact, after resetting the MR-HSRD (by opening the control valve), due to pressure drop between two sides of the cylinder the MR-fluid flows through the MR-valve (in the flow mode). Then, the appropriate magnetic field (according to the pressure drop) is applied to increase the yielding stress of MR-fluid so that most part of stored energy dissipated at the minimum time by shearing the excited MR-fluid. By now, different kinds of external bypass MR-valve are proposed and their characteristics are studied [37-45].

The Bingham plastic theory is used to develop the theoretical model for MR-valve. The flow of the MR-fluid in MR-valve is assumed incompressible. In Figure 6, the schematic of the MR-valve and the velocity profile for the flow of a Bingham fluid in the concentric annulus of MR-valve is shown. The geometric dimensions used in the theoretical formulation based on the axi-symmetric diagram of the annular gap also are shown in Figure 6. When Bingham fluid flows in a concentric annulus, always there is an un-sheared portion of the fluid which moves as a solid plug [46, 47], as illustrated by the velocity profile in Figure 6. The velocity across the plug (u_{plug}) is constant and it is assumed that the pressure difference, Δp, along the entire annulus is insufficient to overcome the yield stress inside this plug. The plug is bounded between $r=a$ and $r=b$, and the values of a and b are unknown.

The existence of a plug flow requires that any shear stress associated with viscosity must be equal to zero inside the plug, as well as on the plug boundaries, *a* and *b*. In Figure 6, the ratio of the inner radius to the outer radius of the annulus is denoted by α and *R* is the outer radius. Any velocity and force vector is assumed to be positive in the direction of the flow. The shear stress in the fluid is represented by the symbol τ_{rx}.

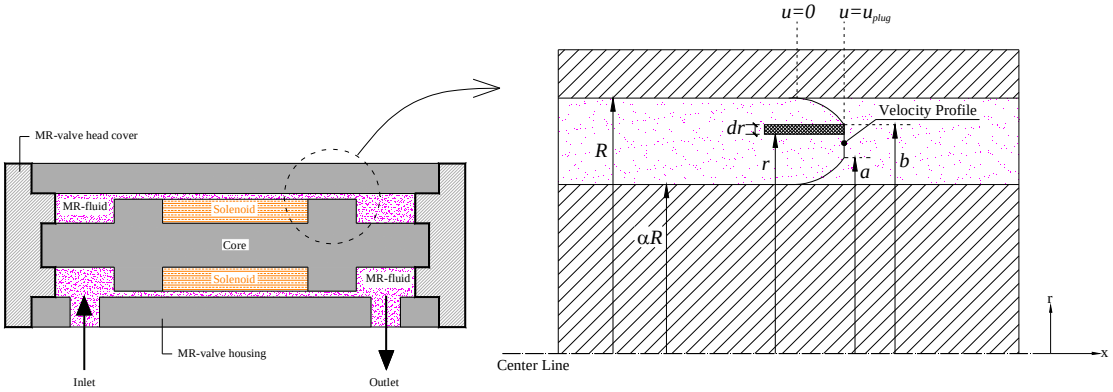

Figure 5. Velocity profile for the flow of fluid with a yield stress in a concentric annulus

A force balance over length *L* of any cylindrical element of the fluid can be written as:

$$d[-2\pi rL\tau_{rx}] = \Delta p \times 2\pi r dr \tag{15}$$

The negative sign on the left-hand side of Eq. (15) is to account for the differential force, which is acting against the direction of flow. Integrating this equation for the region between $r=\alpha R$ and $r=a$ and rearranging the solution in terms of τ_{rx}:

$$\tau_{rx} = -\frac{\Delta p r}{2L} + \frac{A_1}{r} \qquad for \qquad \alpha R \le r \le a \tag{16}$$

Where A_1 is a constant of integration yet to be determined. Using a similar approach for the region between $r=R$ and $r=b$, the shear stress can be written as:

$$\tau_{rx} = \frac{\Delta p r}{2L} + \frac{A_2}{r} \qquad for \qquad b \le r \le R \tag{17}$$

The total shear force at the walls of the annulus is equal to the force exerted by the overall pressure Δp acting on the entire body of fluid inside the annulus, hence:

$$\begin{aligned} &\Delta p \pi (R^2 - \alpha^2 R^2) = 2\pi\alpha RL[\tau_{rx}]_{r=\alpha R} + 2\pi RL[\tau_{rx}]_{r=R} \\ &\Rightarrow \quad \frac{\Delta p R(1-\alpha^2)}{2L} = [\tau_{rx}]_{r=R} + [\tau_{rx}]_{r=R} \end{aligned} \tag{18}$$

Substituting Eq. (16) and (17) for the τ_{rx} term in Eq. (18) gives:

$$\frac{\Delta pR(1-\alpha^2)}{2L} = \alpha[-\frac{\Delta p \alpha R}{2L} + \frac{A_1}{\alpha R}] + [\frac{\Delta pR}{2L} + \frac{A_2}{R}] \;\Rightarrow\; 0 = \frac{1}{R}(A_1 + A_2) \tag{19}$$

A non-trivial (and physically realizable) solution for Eq. (19) is A_1=-A_2. To simplify the formulation, A_1 is replaced by a single constant -A, so that:

$$A_1 = -A \quad and \quad A_2 = A \tag{20}$$

Substituting the Eq. (20) in Eq. (16) and (17):

$$\begin{cases} \tau_{rx} = -(\frac{\Delta pr}{2L} + \frac{A}{r}) & for \quad \alpha R \le r \le a \\ \tau_{rx} = \frac{\Delta pr}{2L} + \frac{A}{r} & for \quad b \le r \le R \end{cases} \tag{21}$$

The total shear force acting on the cylindrical surfaces of the un-sheared annular plug is equals to the pressure difference (Δp) multiplied by the cross sectional area of the plug:

$$\tau_y(2\pi al) + \tau_y(2\pi bl) = \Delta p\pi(b^2 - a^2) \;\Rightarrow\; b - a = \frac{2L\tau_y}{\Delta p} \tag{22}$$

Eq. (22) can be used to compute the minimum pressure difference Δp_{min} required to start the flow where τ_y is the yield stress that acting on cylindrical surfaces of the un-sheared annular plug. Using $a=\alpha R$ and $b=R$, the minimum pressure difference is:

$$\Delta p_{\min} = \frac{2L\tau_y}{R(1-\alpha)} \tag{23}$$

As it is seen in Eq. 23, the minimum pressure difference depends on the yield stress of MR-fluid and the geometric dimensions of annulus of MR-valve. Subsequently, the yield stress of MR-fluid, $\tau_y(H)$, depends on magnetic field. The minimum required force to start the flow of MR-fluid in MR-valve connected to the MR-HSRD can be calculated as:

$$F_{\min} = \frac{2L\tau_y}{R(1-\alpha)} A \tag{24}$$

Where A is the piston area of the MR-HSRD.

In fact, once the MR-HSRD is excited, the resistive force of device can be measured by a load-cell. At the resetting time, when the resistive force is maximum, the controller commands to open the control valve and let the MR-fluid flowing across the MR-valve. Simultaneously, the controller calculates the required yield stress of MR-fluid according to measured resistive force of device by using Eq. (24). Then, by altering the magnetic field in MR-valve, the yield stress is adjusted to its threshold value continuously until most of the stored energy in MR-HSRD is dissipated and the device resistive force return to zero. Afterward, the magnetic field is set to zero (MR-fluid flow in off-state) and device waits for next reset time. All this processes happens in few milliseconds.

4. CONTROL LOGICS

Resettable devices offer the unique opportunity to re-shape the structural hysteresis loop to satisfy design needs. This opportunity is achieved by selecting the opening time and closing time of the control valve. Based on control algorithm, there are a number of points at which the control valve can practically be opened to reset the device. For a straightforward algorithm, these points occur where the piston movement changes direction or crosses an initial zero position. The control valve commands and timing of commands can specify a range of possible device responses. There are three basic control logics based on the control valve commands. In the first control logic (called resetting logic); the control valve is opened for a very short time at the peaks of piston displacements (when the piston velocity is zero). As a result, practically all stored energy is released and dissipated suddenly. For a sinusoidal piston displacement, Figure 7(a) shows the behavior of MR-HSRD when the resetting logic is selected and all stored energy is released at the peak of each sine-wave. As it is seen, the resetting control logic provides damping in all four quadrants of the force-displacement diagram. In the second control logic (called type-1 switching logic), the valve is opened at the peaks of piston displacements and remains in the open status until the piston returns to initial zero position. The force-displacement curves for this logic are shown in Figure 7(b) for a sine-wave. In type-2 switching logic (Figure 7(c)), the valve is opened at the zero position and remains in the open status until the piston reach to peak displacements. The comparison of different control logics in structural response control is reported in reference [16].

The ability to manipulate the overall hysteretic behavior through proper control logic, allows the MR-HSRD to be effectively applied to a much wider range of structural situations as compared to other semi-active and passive devices. Moreover, the control logics are decentralized, as they just require local measurement (e. g. relative displacement or velocity of two ends of device). Since the mass and stiffness properties of the structure do not affect the control logics explicitly, the control law is robust with respect to modeling errors in mass and stiffness properties of the structure or some nonlinearity that may occur.

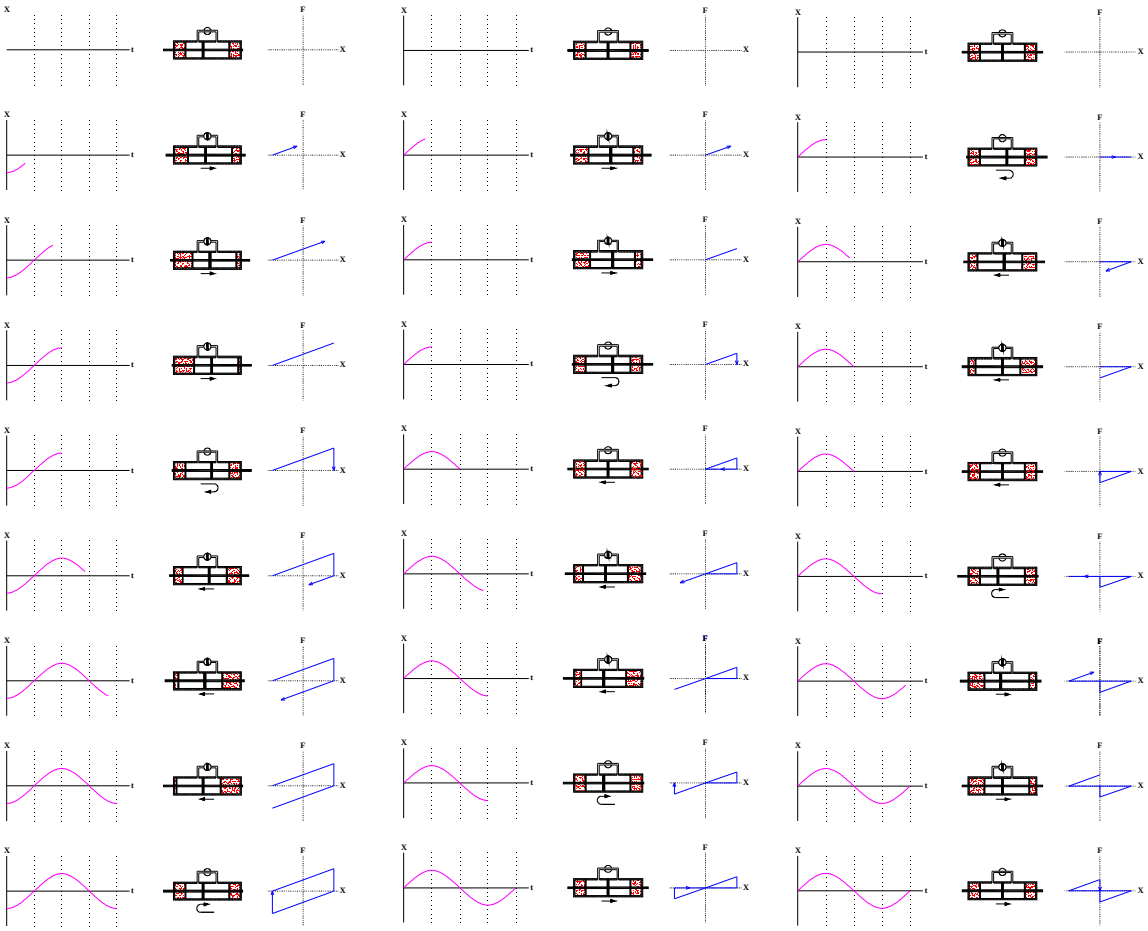

(a) Resetting logic (b) Type-1 switching logic (c) Type-2 switching logic

Figure 6. Schematic of control logics for MR-HSRD

5. TEST SETUP

For evaluating the proposed device and validating the mathematical models, a series of experiments were conducted at the Structural Dynamics Laboratory of the Hong Kong Polytechnic University. For this purpose and to realize the force-displacement relation of the proposed device, the configuration shown in Figure 8 is adopted for MR-HSRD. In the first phase of the experiments, the stiffness of the device is considered and the effects of different parameters that change the stiffness are examined. In this stage, the prototype#1 was manufactured where the air cylinders are split from the main cylinder and are connected to it by high-pressure rubber pipes (Figure 8). Hence, the initial length of the air cylinder (L_{0G}) could be adjusted easily. Furthermore, in the first stage of test, there is not any MR-valve in bypass pipe and a simple on-off manual valve was installed in the bypass pipe. Moreover, the hydraulic oil is used instead of MR-fluid because in this stage, it is not needed to use MR-fluid. The piston diameter (D) of the prototype#1 is chosen 3 cm both for air and main

cylinder. The maximum initial length of the air cylinder (L_{0G}) can be adjusted up to 5 cm depending on required maximum displacement. The manufactured device and test setup photos are shown in Figure 9. The drawing and dimensions of the main cylinder and air cylinder are shown in Figure 10 and Figure 11, respectively.

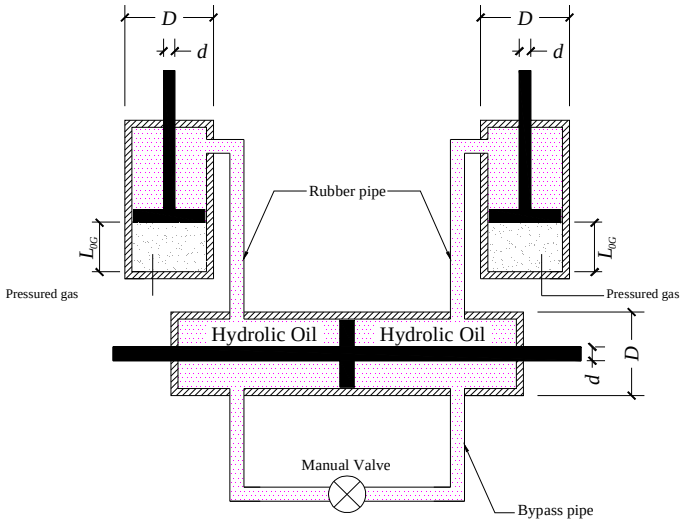

Figure 7. Schematic of the prototype#1

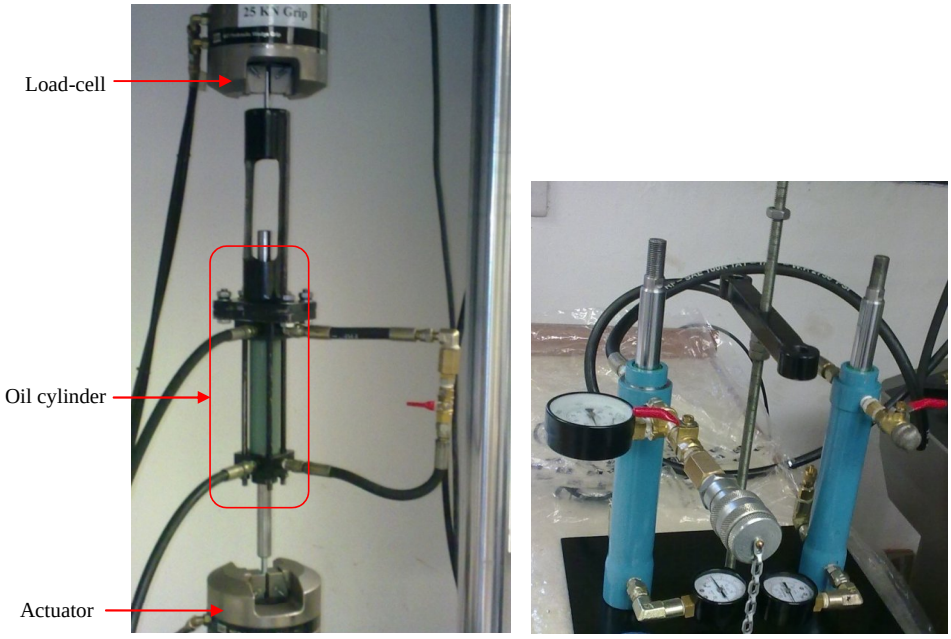

(a) (b)

Figure 8. Test setup of the prototype#1 (a) Main cylinder (oil cylinder) with bypass pipe and the manual control valve (b) Air cylinders and the adjustable stand for changing the length of gas reservoirs

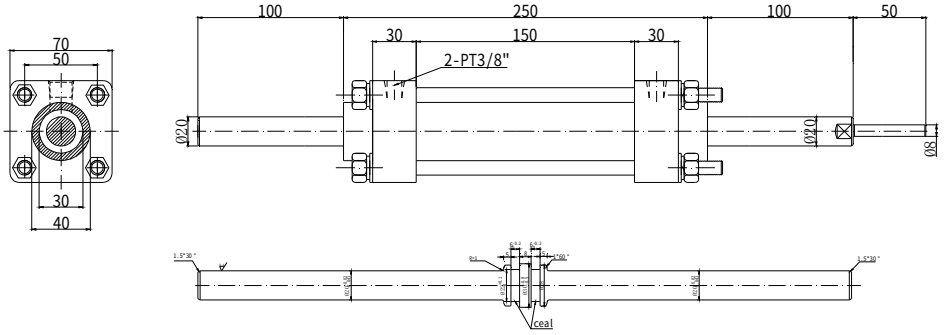

Figure 9. Drawing of main cylinder (all dimensions are in mm)

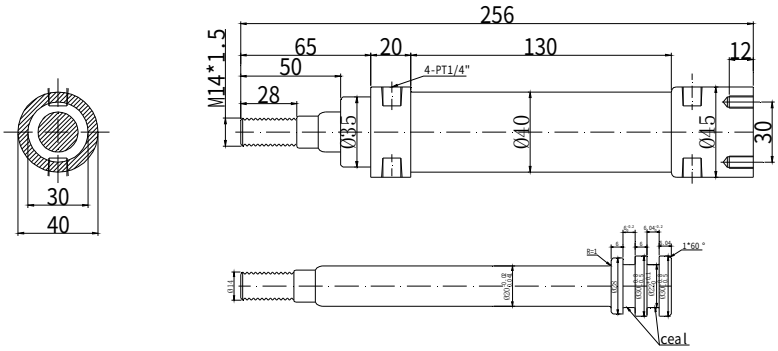

Figure 10. Drawing of air cylinder (all dimensions are in mm)

According to Eq. (11), the effective parameters in linear model of device stiffness are D (piston diameter), p_{0G} (the initial pressure of gas), L_{0G} (the initial length of the gas reservoir) and V_{con} (the constant volume in the gas reservoir). In the prototype#1, among of these four parameters two of them are constant, the piston diameter (D=3 cm) and the constant volume in the gas reservoir (V_{con}=10 cm^3). Therefore, adjusting p_{0G} and L_{0G} can change the device stiffness. The graph of device stiffness K_D versus L_{0G}, for different initial pressures of gas (p_{0G}) is shown in Figure 12. The amounts of linear stiffness of the prototype#1 according to Eq. (11) for different L_{0G} and different p_{0G} are shown in Table 1 as well.

Table 1: Stiffness of theprototype#1 with different L_{0G} and p_{0G}

Device model number	L_{0G} **(cm)**	K_D **(kN/m)**		
		p_{0G} **(kN/m^2)**		
		250	**500**	**600**
Prototype#1	1	20.49	40.98	49.18
	2	14.49	28.98	34.78
	3	11.21	22.42	26.90
	4	9.14	18.28	21.93
	5	7.71	15.43	18.51

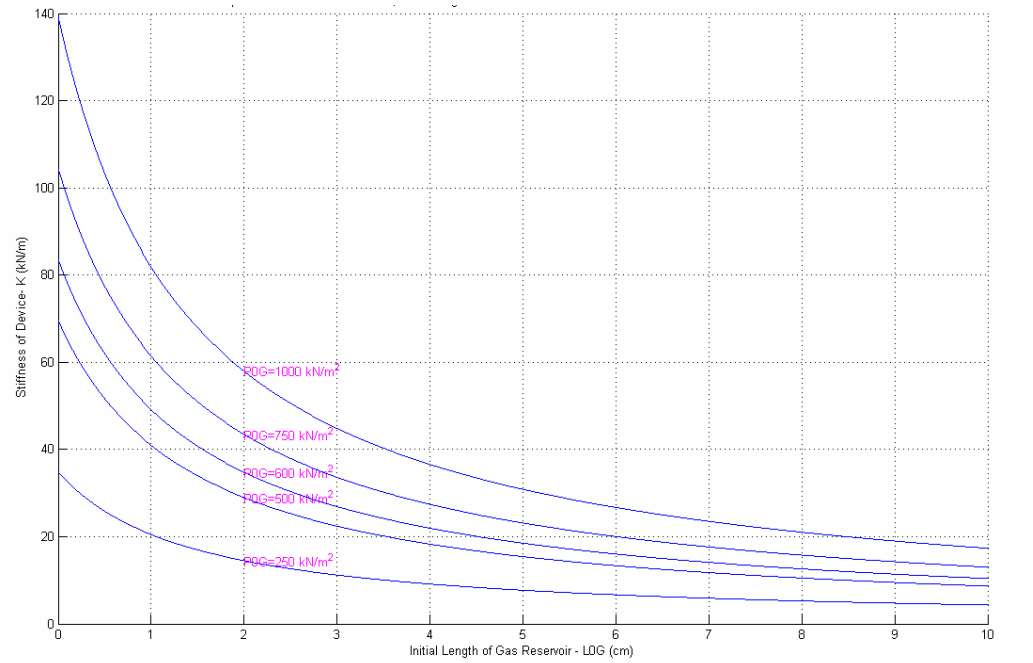

Figure 11. Relation between linear stiffness (K_D) versus L_{0G}, for different initial pressures of gas (p_{0G}) for prototype#1 with D=3 cm and V_{con}=10 cm^3

6. TEST RESULTS

In order to realize the effect of large displacement and high initial gas pressure (p_{0G}) on the device stiffness, the quasi-static test with speed of 1 mm/sec and maximum available displacement of the piston is carried out. The test was conducted for maximum amplitude 4.5 cm with L_{0G}=5 cm and four different gas pressures, p_{0G} =500, 750, 1000, 1250 kN/m^2. To compare the test results with predicted behavior, the force-displacement response is depicted along with linear and nonlinear mathematical model predictions in Figure 13.

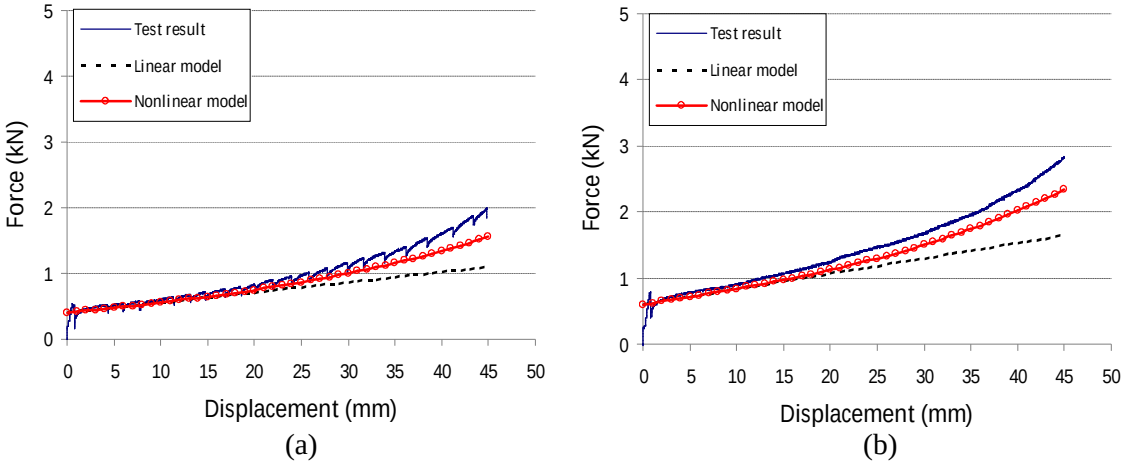

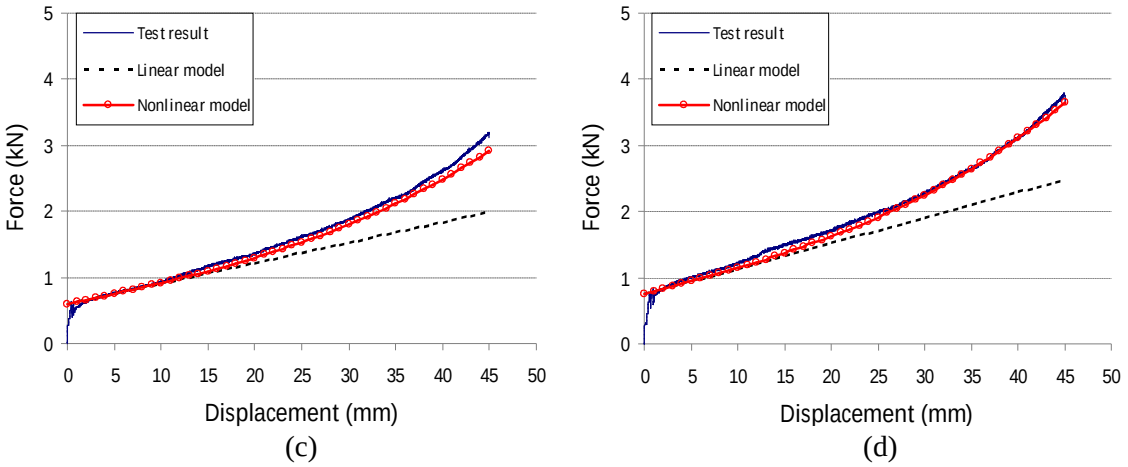

Figure 12. Force-displacement response of prototype#1 and linear and nonlinear model with L_{0G}=5 cm and V_{con}=10 cm^3 for 4.5 cm quasi-static piston motion (a) p_{0G}=500 kN/m^2, (b) p_{0G}=750 kN/m^2, (c) p_{0G}=1000 kN/m^2, d) p_{0G}=1250 kN/m^2

Experimental results are in agreement with the linear relation between the gas pressure and the stiffness of the MR-HSRD for small displacement of piston (less than 50% of the gas reservoir length) as predicted by linear mathematical model (Eq. (11)). However, for relatively large length of the gas reservoir and with increasing displacement, especially in higher pressure, the difference between the linear model and test result increases dramatically. But, the nonlinear model prediction is quite well and has good correlation with test results.

To consider the effect of frequency and amplitude in the device behavior, dynamic tests for sinusoidal displacements with different amplitudes and frequencies are conducted. The device is tested with different initial gas pressures. At each pressure, different air volumes (that can be adjusted by altering the length of the gas reservoir) are considered. The tests are carried out for two valve situations; on-state which valve is close and the device resist against piston displacement and off-state which valve is open. The off-state test is performed to find resistance force due to friction between ceiling rings and moving part and viscose force of the moving oil through the connecting pipes.

The tests are conducted for three different length of gas reservoir (L_{0G}=2, 3 and 4 cm) and three different gas pressures (p_{0G}=250, 500 and 600 kN/m^2). The piston displacements are sinusoidal with three different frequencies (i.e. f=0.1, 0.5 and 1.0 Hz) and different amplitudes. The test results for p_{0G}=500 kN/m^2 and 1 cm amplitude are shown in Figure 14 to Figure 16 for different L_{0G}. As shown in the Figure 14(a), Figure 15(a) and Figure 16(a), the linear model prediction captures most of the device behavior for tested frequencies. Moreover, the test carried out in the off-state valve status. As shown in Figure 14(b), Figure 15(b) and Figure 16(b), the device resistance force is almost constant (about 0.1 kN) in off-state status for tested frequencies regardless of the initial length of the gas reservoir.

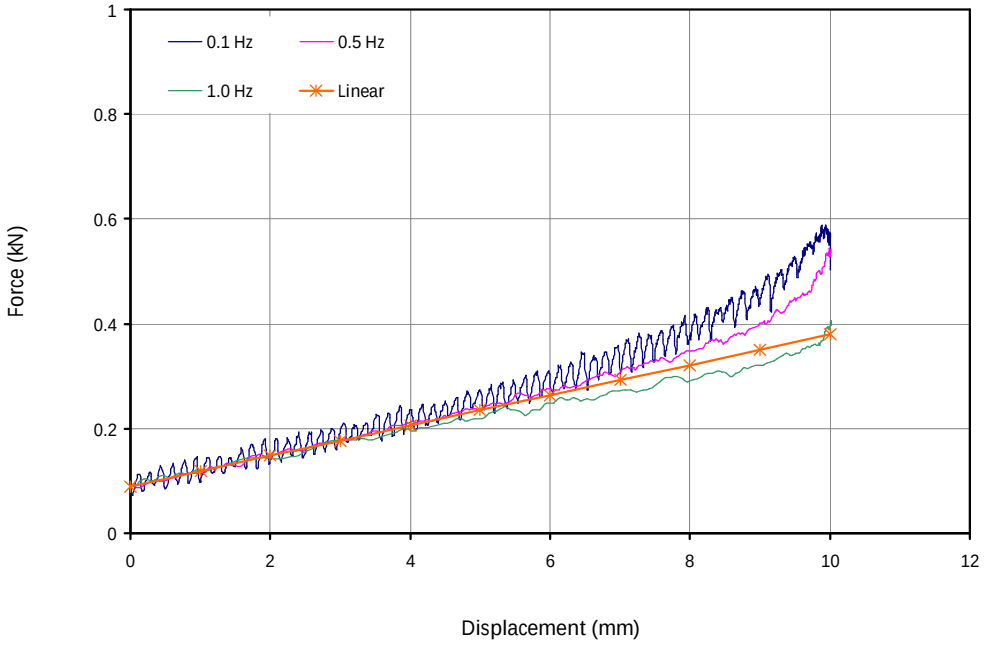

(a)

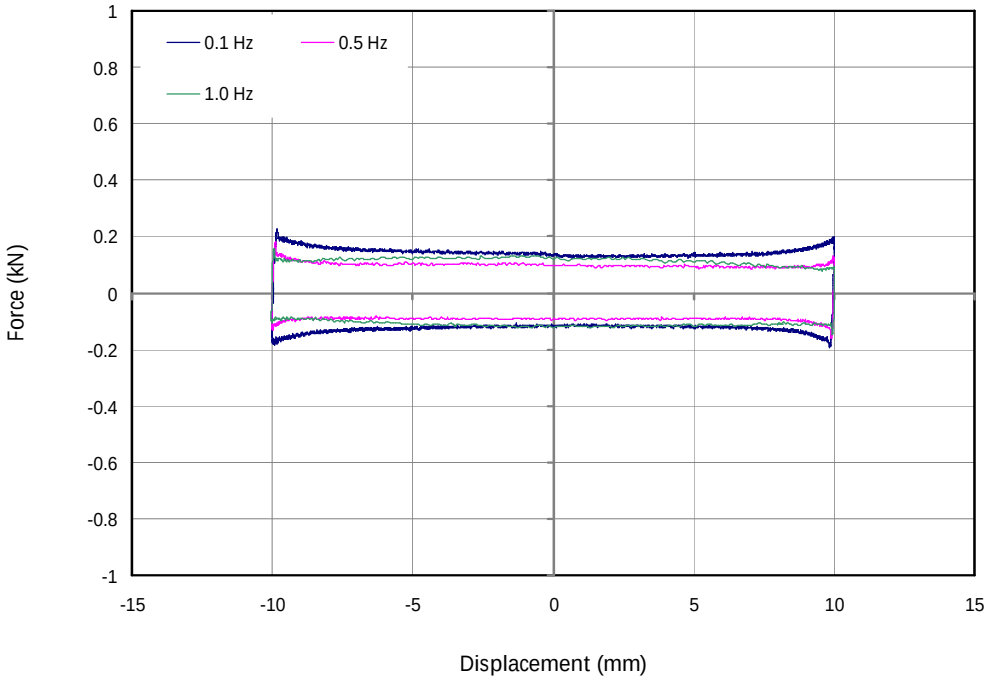

(b)

Figure 13. First quarter force-displacement response of the device with L_{0G}=2 cm, V_{con}=10 cm^3 and p_{0G}=500 kN/m^2 for 1 cm sinusoidal piston motion at 0.1, 0.5 and 1.0 Hz (a) On-state (control valve is close), (b) Off-state (control valve is open)

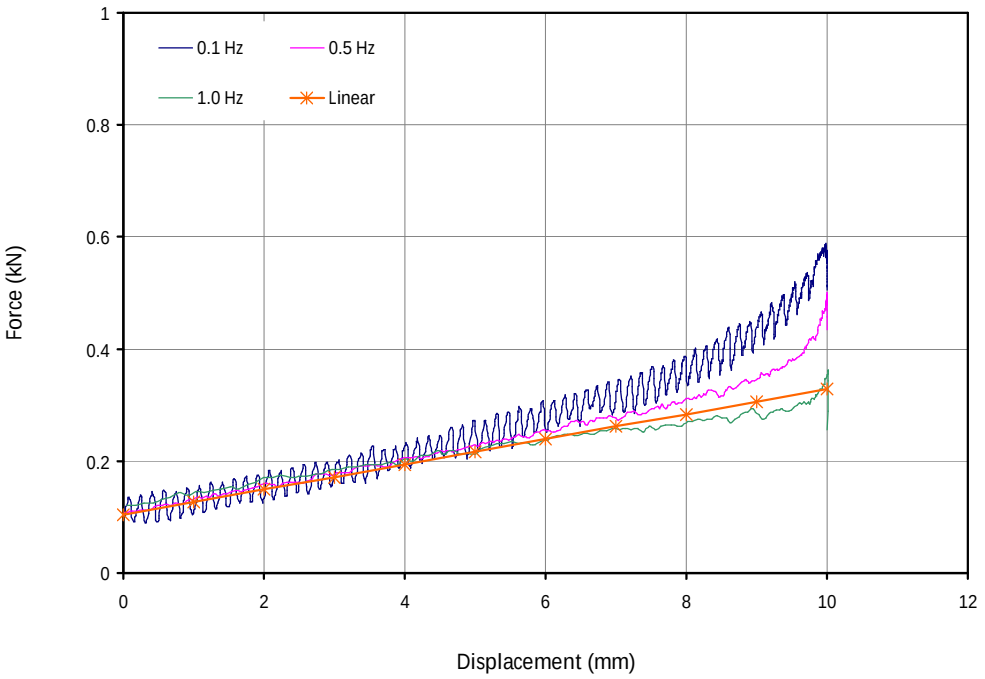

(a)

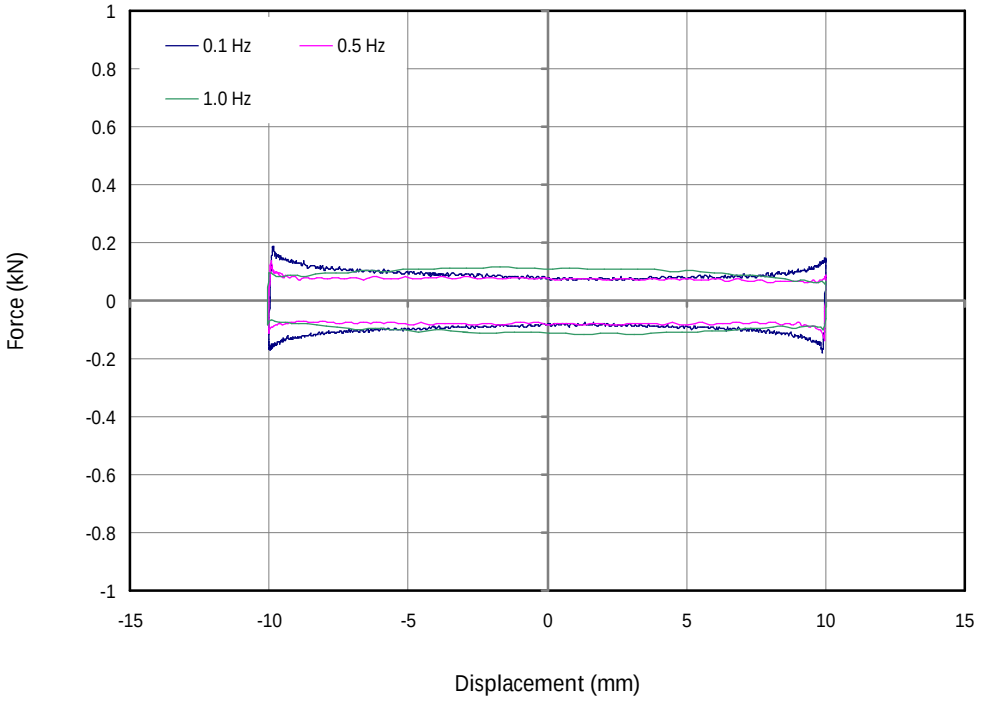

(b)

Figure 14. First quarter force-displacement response of the device with L_{0G} =3 cm, V_{con}=10 cm^3 and p_{0G}=500 kN/m^2 for 1 cm sinusoidal piston motion at 0.1, 0.5 and 1.0 Hz (a) On-state (control valve is close), (b) Off-state (control valve is open)

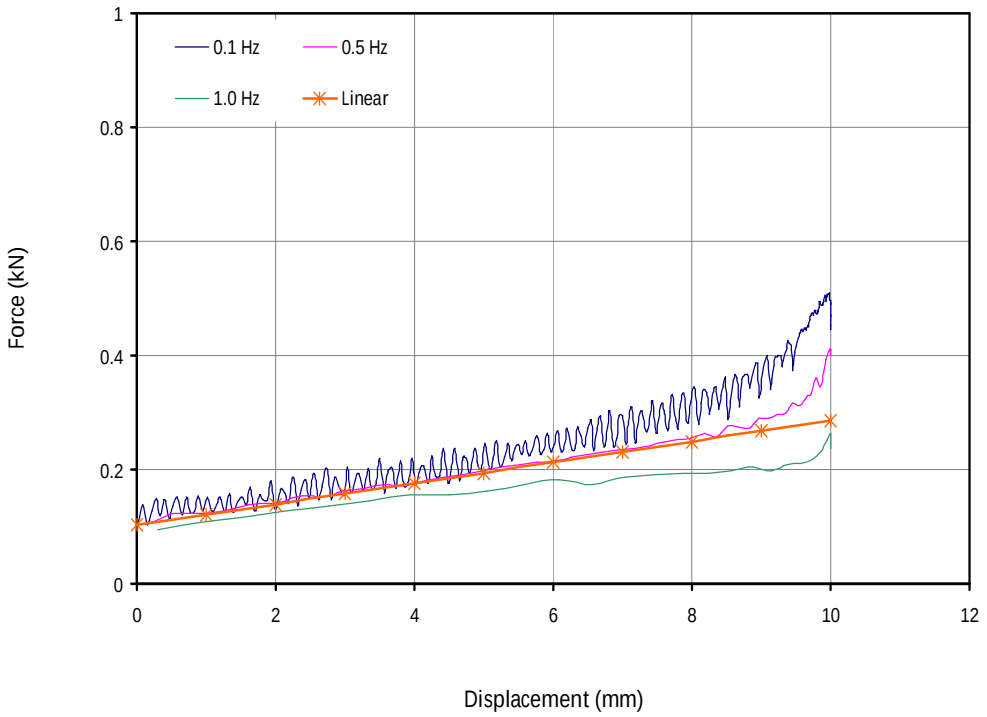

(a)

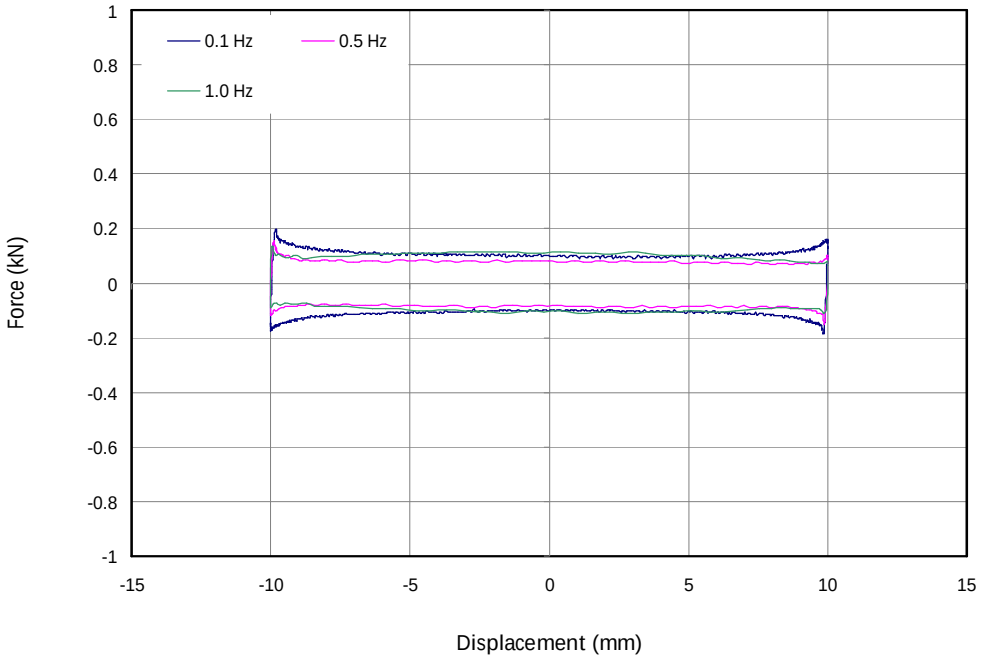

(b)

Figure 15. First quarter force-displacement response of the device with L_{0G} =4 cm, V_{con}=10 cm^3 and p_{0G}=500 kN/m^2 for 1 cm sinusoidal piston motion at 0.1, 0.5 and 1.0 Hz (a) On-state (control valve is close), (b) Off-state (control valve is open)

7. CONCLUSIONS

A new innovative semi-active resettable device by using MR-fluid (MR-HSRD) is introduced and studied. The novel device consists of a cylinder-piston system with a control valve as well as a MR-valve mounted on a bypass pipe connecting two sides of the cylinder. The cylinder has two chambers; each chamber contains two parts, pressured gas and MR-fluid that are separated by a movable piston. The MR-HSRD is set by changing the stiffness and the damping of the device independently. Moreover, the hysteresis behavior can be changed by using different control logics for control valve. Two mathematical models i.e., linear and non-linear models were established for the device force-displacement relation. For evaluating the device performance and validation of the mathematical models, a series of quasi-static and dynamic experiments were carried out. In the first phase of the experiments, the quasi-static and dynamic tests were conducted at various lengths of gas reservoir (L_{0G}) and gas pressure (p_{0G}). The following conclusions can be drawn based on the test results of the first phase:

- Experimental results show a linear relation between the gas pressure and the stiffness of the MR-HSRD for small displacement of piston (less than 50% of the gas reservoir length) as predicted by linear mathematical model.
- For the large displacement of the piston (more than 50% of the gas reservoir length), the linear model cannot depict device behavior well and the difference between the linear model and device behavior increase dramatically. But the nonlinear model prediction is quite well and has good correlation with device behavior.
- The behavior of the device in off-state (control valve open) is quite same for tested frequencies and it is almost constant (about 0.1 kN).
- Significant changes in the stiffness of the device can be obtained by adjusting either the initial pressure of gas (p_{0G}) or the initial length of the gas reservoir (L_{0G}). It makes the device adaptable for different structural control situations.

Acknowledgements: The work presented in this paper was supported by The Shahrood University of Technology and The Hong Kong Polytechnic University under the grant H-ZG27. These supports are gratefully acknowledged.

REFERENCES

1. 1. Spencer BF, Nagarajaiah S. State of the art of structural control, *Journal of Structural Engineering, ASCE*, **129**(2003) 845–56.
2. Jabbari F, Bobrow JE. Vibration suppression with resettable device, *Journal of Engineering Mechanics, ASCE*, **128**(2002) 916–24.
3. Bobrow JE, Jabbari F, Thai K. An active truss element and control law for vibration suppression, *Smart Materials and Structures*, **4**(1995) 264–9.
4. Kurino H, Tagami J, Shimizu K, Kobori T. Switching oil damper with built-in controller for structural control, *Journal of Structural Engineering, ASCE*, **129**(2003) 895–904.

5. Kurino H, Matsunaga Y, Yamada T, Tagami J. High performance passive hydraulic damper with semi-active characteristics, *Proceeding of the 13th World Conference on Earthquake Engineering (13WCEE)*, Vancouver, BC, Canada, (2004).
6. Chase J, Mulligan K, Gue A, Alnot T, Rodgers G, Mander J, Elliott R, Deam B, Cleeve L, Heaton D. Re-shaping hysteretic behaviour using semi-active resettable device dampers, *Engineering Structures*, **28**(2006) 1418–29.
7. Nagarajaiah S, Reinhorn A, Constantinou M, Taylor D. Variation of supplemental stiffness and damping using adaptive fluid spring and damper (ASD), *Proceeding of the NSF Engineering Research and Innovation Conference*, Honolulu, Hawaii, USA, 2009.
8. Bobrow JE, Jabbari F, Thai K. A new approach to shock isolation and vibration suppression using a resetable actuator, *Journal of Dynamic Systems Measurement and Control-Transactions of the ASME*, **122**(2000) 570–3.
9. Yang JN, Bobrow J, Jabbari F, Leavitt J, Cheng CP, Lin PY. Full-scale experimental verification of resetable semi-active stiffness dampers, *Earthquake Engineering and Structural Dynamics*, **36**(2007) 1255–73.
10. Barroso LR, Chase JG, Hunt S. Resettable smart dampers for multi-level seismic hazard mitigation of steel moment frames, *Journal of Structural Control*, **10**(2003) 41–58.
11. Leavitt J, Bobrow JE, Jabbari F, Yang JN. Application of a high-pressure gas semi-active resettable damper to the benchmark smart base-isolated building, *Structural Control and Health Monitoring*, **13**(2006) 748–57.
12. Yang JN, Kim JH, Agrawal AK. Resetting semiactive stiffness damper for seismic response control, *Journal of Structural Engineering, ASCE*, **126**(2000) 1427–33.
13. Yang JN, Agrawal AK. Semi-active hybrid control systems for nonlinear buildings against near-field earthquakes, *Engineering Structures*, **24**(2002) 271–80.
14. Djajakesukma SL, Samali B, Nguyen H. Study of a semi-active stiffness damper under various earthquake inputs, *Earthquake Engineering & Structural Dynamics*, **31**(2002) 1757–76.
15. Shimizu K, Yamada T, Tagami J, Kurino H. Vibration tests of actual buildings with semi-active switching oil damper, *Proceeding of the 13th World Conference on Earthquake Engineering (13WCEE)*, Vancouver, BC, Canada, 2004.
16. Rodgers GW, Mander JB, Chase JG, Mulligan KJ, Deam BL, Carr A. Re-shaping hysteretic behaviour-spectral analysis and design equations for semi-active structures, *Earthquake Engineering & Structural Dynamics*, **36**(2007) 77–100.
17. Mulligan KJ, Chase JG, Mander JB, Rodgers GW, Elliott RB, Franco-Anaya R, Carr AJ. Experimental validation of semi-active resetable actuators in a 1/5th scale test structure, *Earthquake Engineering and Structural Dynamics*, **38**(2009) 517–36.
18. Mulligan KJ, Fougere M, Mander JB, Chase JG, Deam BL, Danton G, Elliot RB. Hybrid experimental analysis of semi-active rocking wall systems, *Proceeding of the New Zealand Society for Earthquake Engineering Conference- Remembering Napier 1931, Building on 75 Years of Earthquake Engineering in New Zealand (2006 NZSEE)*, Napier, New Zealand, 2006.
19. Chase JG, Rodgers GW, Mulligan KJ, Mander JB, Dhakal RP. Probabilistic analysis and non-linear semi-active base isolation spectra for aseismic design, *Proceeding of the*

8th Pacific Conference on Earthquake Engineering (8PCEE), Singapore, 2007.
20. Chey MH, Carr AJ, Chase JG, Mander JB. Resetable tuned mass damper and its application to isolated stories building system, *Proceeding of the 14th World Conference on Earthquake Engineering (14WCEE)*, Beijing, China, 2008.
21. Franco-Anaya R, Carr AJ, Chase JG. Semi-active resettable devices for seismic protection of civil engineering structures, *Proceeding of the 14th World Conference on Earthquake Engineering (14WCEE)*, Beijing, China, 2008.
22. Mulligan KJ, Chase JG, Mander JB, Elliot R. Semi-active resetable actuators incorporating a high pressure air source, *Proceeding of the New Zealand Society for Earthquake Engineering Conference*-Performance by Design-Can We Predict It? (2007 NZSEE), Palmerstone North, New Zealand, 2007.
23. Mulligan KJ, Chase JG, Mander JB, Rodgers GW, Elliott RB. Nonlinear models and validation for resetable device design and enhanced force capacity, *Structural Control and Health Monitoring*, **17**(2010) 301–16.
24. Thai K, Jabbari F, Bobrow JE. Structural control via semi-active and hybrid control, *Proceeding of the American Control Conference*, Albuquerque, New Mexico, USA, (1997), pp. 6-10.
25. Bobrow JE, Jabbari F. A high-performance semi-active controller for structural vibration suppression, *Smart Structures and Integrated Systems - Smart Structures and Materials*, **3041**(1997) 67–74.
26. Leavitt J, Jabbari F, Boborw JE. Optimal control and performance of variable stiffness devices for structural control, *Proceeding of the American Control Conference (ACC)*, Portland, OR, USA, 2005, pp. 2499-2504.
27. Leavitt J, Jabbari F, Bobrow JE. Optimal performance of variable stiffness devices for structural control, *Journal of Dynamic Systems, Measurement, and Control*, **129**(2007) 171–7.
28. Agrawal AK, He WL. Control of seismically excited cable-stayed bridge using a resetting semi-active stiffness damper, *Proceeding of the American Control Conference (ACC)*, Arlington, VA, USA, 2001, pp. 1103-1108.
29. Agrawal AK, Yang JN, He WL. Applications of some semiactive control systems to benchmark cable-stayed bridge, *Journal of Structural Engineering, ASCE*, **129**(2003) 884–94.
30. Samali B, Djajakesukma SL, Nguyen H. Effectiveness of semi-active stiffness damper in a five-storey model, *Computational Mechanics*, **1**(2001) 1425–30.
31. Chen XQ, Chase JG, Mulligan KJ, Rodgers GW, Mander JB. Novel controllable semiactive-devices for reshaping structural response, *IEEE-ASME Transactions on Mechatronics*, **13**(2008) 647–57.
32. Mulligan K. *Experimental and analytical studies of semi-active and passive structural control of buildings*, Ph.D. Thesis in Mechanical Engineering, University of Canterbury, Christchurch, New Zealand, 2007.
33. Chase JG, Mulligan KJ, Gue A, Mander JB, Alnot T, Rodgers G, Deam B, Cleeve L, Heaton D. Resetable devices with customized performance for semi-active seismic hazard mitigation of structures, *Proceeding of the New Zealand Society for Earthquake Engineering Conference- Planing and Engineering for Performance in Earthquakes*

(2005 NZSEE), Taupo, New Zealand, 2005.
34. LordCorporation. *Online technical library*. Available from: http://www.lord.com/.
35. Bell RC, Zimmerman DT, Wereley NM, Impact of Nanowires on the Properties of Magnetorheological Fluids and Elastomer Composites, in Electrodeposited Nanowires and Their Applications, Lupu N, Editor. 2010, INTECH.
36. Jolly MR, Bender JW, Carlson JD. Properties and applications of commercial magnetorheological fluids, *Journal of Intelligent Material Systems and Structures*, **10**(1999) 5–13.
37. Wang DH, Ai HX, Liao WH. A magnetorheological valve with both annular and radial fluid flow resistance gaps, *Smart Materials and Structures*, No. 11, **18**(2009) 115001.
38. Wang X, Gordaninejad F, Hitchcock G, Bangrakulur K, Fuchs A, Elkins J, Evrensel C, Dogruer U, Ruan S, Siino M, Kerns M. A new modular magneto-rheological fluid valve for large-scale seismic applications, *Proceeding of the Smart Structures and Materials 2004: Damping and Isolation*, San Diego, CA, USA, 2004, pp. 226–237.
39. Grunwald A, Olabi AG. Design of magneto-rheological (MR) valve, *Sensors and Actuators a-Physical*, **148**(2008) 211–23.
40. Gordaninejad F, Wang X, Hitchcock G, Bangrakulur K, Ruan S, Siino M. Modular high-force seismic magneto-rheological fluid damper, *Journal of Structural Engineering, ASCE*, **136**(2010) 135–43.
41. Hitchcock GH, Wang X, Gordaninejad F. A new bypass magnetorheological fluid damper, *Journal of Vibration and Acoustics*, **129**(2007) 641–7.
42. Aydar G, Wang X, Gordaninejad F. A novel two-way-controllable magneto-rheological fluid damper, *Smart Materials and Structures*, **19**(2010) 065024.
43. Sahin H, Liu Y, Wang X, Gordaninejad F, Evrensel C, Fuchs A. Full-scale magnetorheological fluid dampers for heavy vehicle rollover, *Journal of Intelligent Material Systems and Structures*, **18**(2007) 1161–7.
44. Yoo JH, Wereley NM. Design of a high-efficiency magnetorheological valve, *Journal of Intelligent Material Systems and Structures*, **13**(2002) 679–85.
45. Hitchcock GH, Gordaninejad F, Wang XJ. A new by-pass, fail-safe, magneto-rheological fluid damper, *Proceeding of the SPIE Conference on Smart Materials and Structures*, San Diego, US, 2002.
46. Chooi W, Oyadiji S. Design, modelling and testing of magnetorheological (MR) dampers using analytical flow solutions, *Computers and Structures*, **86**(2008) 473–82.
47. Chhabra RP, Richardson JF. *Non-Niotonian Flow in the Process Industries Fundamentals and Engineering Applications*, Butterworth-Heinemann, Woburn, MA, US, 1999.